RAPID ONSET OXIDATIVE MYOCARDIAL INSULT AND LOSS OF CARDIAC FUNCTION CAUSED BY CONDITIONAL DELETION OF *DICER* IN THE ADULT MURINE HEART CAN BE RESCUED BY ANTI-miRNA-15B STRATEGY

Authors: Jaideep Banerjee*, Sashwati Roy*, Surya C. Gnyawali, Savita Khanna, Guanglong He, Douglas Pfeiffer, Jay L. Zweier, Chandan K Sen.

* *contributed equally*

Affiliation: Davis Heart and Lung Research Institute and Department of Surgery, The Ohio State University Medical Center, Columbus, OH 43210, USA.

Abstract

Background- Dicer endonuclease, critical for maturation of microRNAs (miRNAs), is depleted in heart failure patients with certain forms of cardiomyopathy. We sought to elucidate the mechanisms underlying the rapid loss of cardiac function following cardiac-specific *Dicer* deletion in adult mice. ***Methods and Results-*** Conditional *Dicer* deletion was achieved by a tamoxifen-inducible Cre recombinase in the adult murine myocardium. Heart function, determined using MRI and echocardiography, showed rapid and significant ($p<0.05$, n=5) decrease in fractional shortening, compromised ejection fraction, and increased left ventricular mass. Decreased respiratory control ratio (RCR) noted in isolated heart mitochondria ($p<0.05$, n=5), faster nitroxide radical decay in EPR spectroscopy ($p<0.05$, n=3), along with elevated lipid peroxidation ($p<0.05$, n=3), glutathione oxidation ($p<0.05$, n=4) and lactate ($p<0.05$, n=4) indicated mitochondrial dysfunction and oxidant stress. Microarray and QPCR detected early onset changes in 22 miRNAs ($p<0.05$, n=3) including elevated miRNA-15b. Over expression of miRNA15b in cardiomyocytes, resulted in compromised mitochondrial membrane potential

(measured by TMRM fluorescence and JC-1 flow cytometry, $p<0.05$, n=4). ***Conclusions***- Acute depletion of *Dicer* in adult mice results in miRNA-15b dependent mitochondrial dysfunction and oxidative stress which is followed by rapid loss of cardiac function.

INTRODUCTION

Dicer depletion resulting in arrest of microRNA (miRNA) maturation is known to perturb cardiac development[1-2] and cause pathological consequences[3-4]. Significance of such observations is heightened by the report that Dicer deficiency is associated with specific forms of cardiomyopathy and heart failure in humans[4]. We sought to develop first understanding of the pivotal pathways that initiate cardiac hypertrophy and failure in response to targeted *Dicer* deletion in the adult murine heart. Our strategy has been to delineate primary causative mechanisms by focusing on early onset changes in the adult heart following *Dicer* deletion, with the goal to be able to rescue using miRNA-directed intervention. This approach resulted in the identification of elevated miRNA-15b in the heart as a causative factor. Taken together with the observation that most types of human heart failure are associated with elevated miRNA-15b[5-6], our findings recognize suppression of inducible miRNA-15b as a key approach worthy of therapeutic consideration.

MATERIALS AND METHODS

Development of the transgenic mice. Mice homozygous for *Dicer*-floxed (loxP) alleles and transgenic B6129-Tg (Myh6-cre/Esr1)1Jmk/J were crossed to generate double transgenic (Myh6-cre/Esr1-Dicer$^{fl/fl}$) mice. Adult male mice at 8 weeks of age (Myh6-cre/Esr1-Dicer$^{fl/fl}$ and control Dicer$^{fl/fl}$) were treated with vehicle (10%/90% vol/vol ethanol/corn oil) or tamoxifen (20mg/kg body weight per day diluted in 10%/90% vol/vol ethanol/corn oil) by daily intraperitoneal injections for consecutive 5 days. **Measurement of cardiac function.** MRI and

echocardiography image acquisition and analysis was performed on all mice at the age of 8 weeks (17-21g) as described previously[7]. **miRNA profiling.** Total RNA including miRNA was isolated using mirVana™ miRNA isolation kit and comprehensive profiling of all the mouse/rat miRs annotated in the miRBase 8.0 was performed using the FlexmiR™ MicroRNA Labeling Kit and the Luminex 200 analyzer system. **Combined miRNA / total RNA isolation and reverse transcription.** Total RNA, including miRNA, was isolated using mirVana™ miRNA isolation kit. Specific Taqman assays for miRNA and mirVana qRT-PCR miRNA RT Kit were used with real-time PCR system and Taqman universal master mix. Levels of miRNA were quantified with the relative quantification method using snoRNA202 as the housekeeping miRNA. **Measurement of in vivo tissue redox status with localized electron paramagnetic resonance (EPR).** In vivo tissue redox status was determined by EPR as described previously with modifications[8]. Briefly, 2, 2, 5, 5-tetramethyl-3-carboxylpyrrolidine-*N*oxyl (PCA) was employed as the spin probe to generate a three-line EPR spectrum. The nitroxide solutions were prepared in PBS and kept frozen until use. PCA solution (10 mM, 20 μl) was intramuscularly injected into the left ventricular region. EPR spectra were acquired with a surface loop resonator placed on top of the heart. The lower field peak-height was monitored with time to determine the rate of probe reduction. **TBARS assay.** As a marker of lipid peroxidation in the myocardial tissue, malondialdehyde (MDA) levels were detected by the thiobarbituric acid reactive substances (TBARS) method as reported previously[9] with some modifications (details in supplementary text). **Reduced (GSH) and oxidized (GSSG) glutathione assay**. GSH and GSSG were detected in the heart tissues using an HPLC coulometric electrode array detector (CoulArray Detector, model 5600 with 12 channels; ESA Inc., Chelmsford, MA, USA) as described previously[10-12]. **Lactate measurement.** Mice were euthanized; hearts were dissected

out and homogenized in the assay buffer provided with the Lactate Assay Kit (Biovision). Assay for lactate was done according to the protocol provided with the kit. **Preparation and incubation of mitochondria and measurement of respiration**. Mitochondria extraction was done as published previously[13] with modifications. Respiration rates of cardiac mitochondria were determined immediately following isolation using a Clark oxygen electrode and an oxygen monitor (Yellow Springs Instrument, Yellow Springs, OH) as previously described[14] with slight modifications. All measurements were completed within 1 h. Succinate (10mM) was used as substrate. State 3 respiration rates (ADP-dependent oxygen consumption) were determined following the addition of 200 µM ADP, whereas the rates measured following the consumption of ADP as it was converted to ATP were taken as the state 4 respiration rates (ADP-independent oxygen consumption). Respiratory Control Ratio (RCR) was calculated as a ratio of State 3 to State 4 respiration. **Cell culture.** Murine HL1 cardiomyocytes[15] were cultured in flasks coated with 12.5µg/ml fibronectin and 0.02% gelatin maintained in Complete Claycomb Medium supplemented with 100µM norepinephrine (consisting of 10mM Norepinephrine dissolved in 0.3 mM L-ascorbic acid), 4mM L-glutamine, 10% fetal calf serum, 100 units/ml penicillin and 100µg/ml streptomycin at 37ºC in a humidified atmosphere of 95% air and 5% CO_2. **MiRNA delivery to cells**. Transfection of HL-1 cardiomyocytes was performed as described[16]. Briefly, HL-1 cells (0.15×10^6 cells per well in 12-well plate) were seeded in antibiotic-free supplemented Claycomb medium 24 h before transfection. DharmaFECT 1 transfection reagent was used to transfect cells with hsa-miRNA-15b mimic as per the manufacturer's instructions. Transfection of miRNA mimic negative controls was performed for the control groups. Cells were harvested after 72 h of such treatment. **Measurement of mitochondrial membrane potential (ΔΨ).** *JC-1 assay* Mitochondrial membrane potential changes were assessed using the

lipophilic cationic dye JC-1 as reported previously[17]. Results (percentage of negative cells) were normalized to either non-transfected cells or cells transfected with the scrambled mimic control while CCCP treated cells were used as a positive control. *TMRM assay* Mitochondrial membrane $\Delta\Psi$ was measured using the fluorescent lipophilic cationic dye TMRM, which accumulates within mitochondria in a potential dependent manner[18]. HL1 cells transfected with mir-15b mimic and after 72 h were reseeded on glass coverslips. Following 24 h of re-seeding, the cells were stained with 8 nM TMRM and 0.5 ml/ml plasma membrane potential indicator (PMPI) for 30 min at 37ºC in the dark. Cells were washed with PBS, and digital images of stained live cells were collected using a Zeiss Axiovert 200M microscope[19]. **Western blots.** Western blot was performed as described previously[20-22]. Primary antibodies against Dicer (1:400), Pim1 (1:500) and GAPDH (1:10,000) were used to detect these antigens. **Statistical analyses.** Data are reported as mean ± S.D. of at least three independent experiments as indicated in respective figure legends. Difference between means was tested by Student's *t*-test. Comparisons between multiple groups were made by analysis of variance. $p<0.05$ was considered statistically significant.

RESULTS

Cardiac specific *Dicer* deletion leads to cardiac hypertrophy and impaired cardiac function

To develop double transgenic Myh6-cre/Esr1-Dicer$^{fl/fl}$ mice, floxed *Dicer* allele[23] were bred with mice expressing a tamoxifen-inducible Cre recombinase protein flanked on each end with a mutated murine estrogen receptor ligand binding domain, under the control of the cardiac-specific murine alpha-myosin heavy chain (Myh6) promoter. Intraperitoneal tamoxifen injection (once daily, 5 consecutive days) to adult mice activated Cre recombinase resulting in *Dicer* null mice (Dicer$^{-/-}$). The control set (Dicer$^{+/+}$) was generated by injecting littermates with equivalent

amount of vehicle (ethanol/corn oil) (Figure. 1A). Within 7 days from the start of tamoxifen delivery, Dicer protein was reduced by 70% (Figure 1B) and $Dicer^{-/-}$ mice displayed impaired gait and inactivity compared with $Dicer^{+/+}$ mice. Such evidence was not noted in wild-type mice injected with matched dose of tamoxifen (not shown). Targeted Dicer deletion in the adult murine heart resulted in increased left ventricular myocardial mass and compromised cardiac function as determined by 11.7T MRI and M-mode echocardiography (Figure 1C). Long and short axis serial MR images demonstrated enlarged diastole in $Dicer^{-/-}$ mice indicative of dilated cardiomyopathy (Figure 1D and E and supplementary movie 1 and 2). Objective assessment of the MRI and echocardiography data consistently demonstrated significant ($p<0.05$, n=5) decline in cardiac function as manifested by decreased fractional shortening and lower ejection fraction. Hypertrophy was indicated by a significant increase in the left ventricular mass and wall thickness (Figure 1F and G). Thus, *Dicer* deletion in 8 week old adult mice caused early onset (1 week) hypertrophy and marked loss of cardiac function.

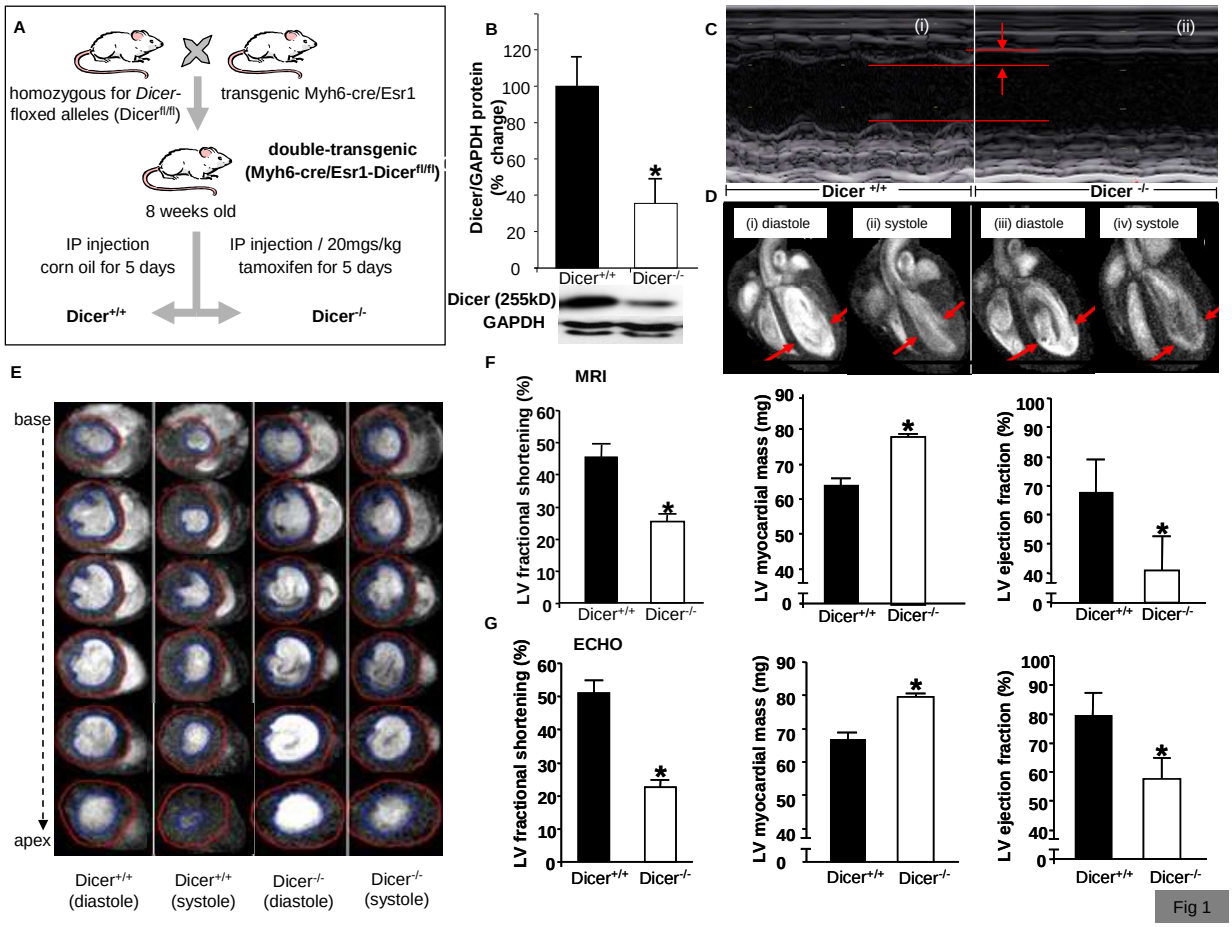

Figure 1. Conditional deletion of the mouse gene *Dicer* and measurement of cardiac functions. (A) Generation of Myh6-cre/Esr1-Dicer$^{fl/fl}$ mice. **(B)** Western Blot showing reduced Dicer expression following tamoxifen injection. **(C)** Representative M-mode images of Dicer$^{+/+}$ and Dicer$^{-/-}$ mice. The data indicates decreased contractility and increased left ventricular (LV) internal dimensions in Dicer-/- mice **(D)** 11.7T MRI images of long axis at diastole (i & iii), systole (ii & iv) cardiac 11.7T MRI images in Dicer$^{+/+}$ and Dicer$^{-/-}$ mice. The diastole of Dicer$^{-/-}$ mice was enlarged due to insufficient contraction of the heart (shown by arrows). **(E)** 11.7T images of short axis at diastole and systole of 1.0 mm slices stacked along columns from base to apex of the left ventricle of both Dicer$^{+/+}$ and Dicer$^{-/-}$ mice. Blue contour lines indicate LV volume. Quantification of LV fractional shortening, LV myocardial mass, and LV ejection fraction (EF) by MRI **(F)** and ECHO **(G).** Data are expressed as mean ± SD (n=5). Data indicates decreased LV fractional shortening and EF and increased LV myocardial mass in Dicer$^{-/-}$ mice. Solid bars represent Dicer$^{+/+}$ and open bars represent Dicer$^{-/-}$.

Cardiac specific *Dicer* deletion leads to early onset changes in specific miRNAs

MiRNA microarray studies identified a limited set of 22 miRNAs (out of 327 listed in miRbase 8.0; 6.7%) which significantly changed (p<0.05, n=3) after the first week of tamoxifen injection when over 50% of cardiac function was already compromised. The strategy was to study an early time point so that the primary mediators of cardiac dysfunction could be unveiled. Of the 22 candidate miRNAs identified, only 5 were elevated while 17 were down-regulated. Microarray results were confirmed using QPCR (Figure 2A-C). Of the miRNAs elevated following Dicer deletion, miRNA-15b was a key candidate predicted to target mitochondrial function as determined by TargetScan^{TM} v 5.1 and Pictar^{TM}. Indeed, delivery of miR-15b to cardiomyocytes specifically compromised mitochondrial membrane potential (TMRM fluorescence) (Fig. 3A and B). Mitochondrial membrane potential changes assessed using the JC-1 assay demonstrated that over expression of miRNA-15b in cardiomyocytes compromised $\Delta\Psi$ (Fig. 3C and D).

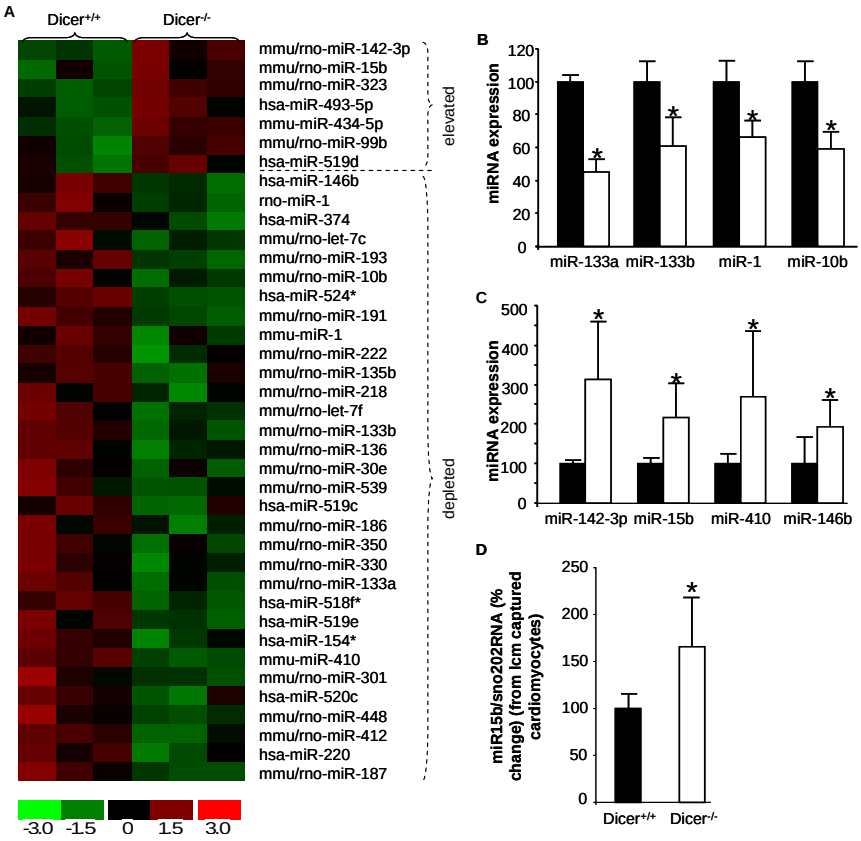

Figure 2. Differential expression of miRNAs on targeted *Dicer* deletion. (A) Heat map generated for the differentially expressed miRNAs in Dicer$^{+/+}$ and Dicer$^{-/-}$ mice. **(B)** Validation of selected miRNAs by real-time PCR showing (i) down regulated miRNAs and (ii) up regulated miRNAs in Dicer$^{-/-}$ (open bars) as opposed to Dicer$^{+/+}$ (solid bars). Data are expressed as mean ± SD (n=5).

Fig 2

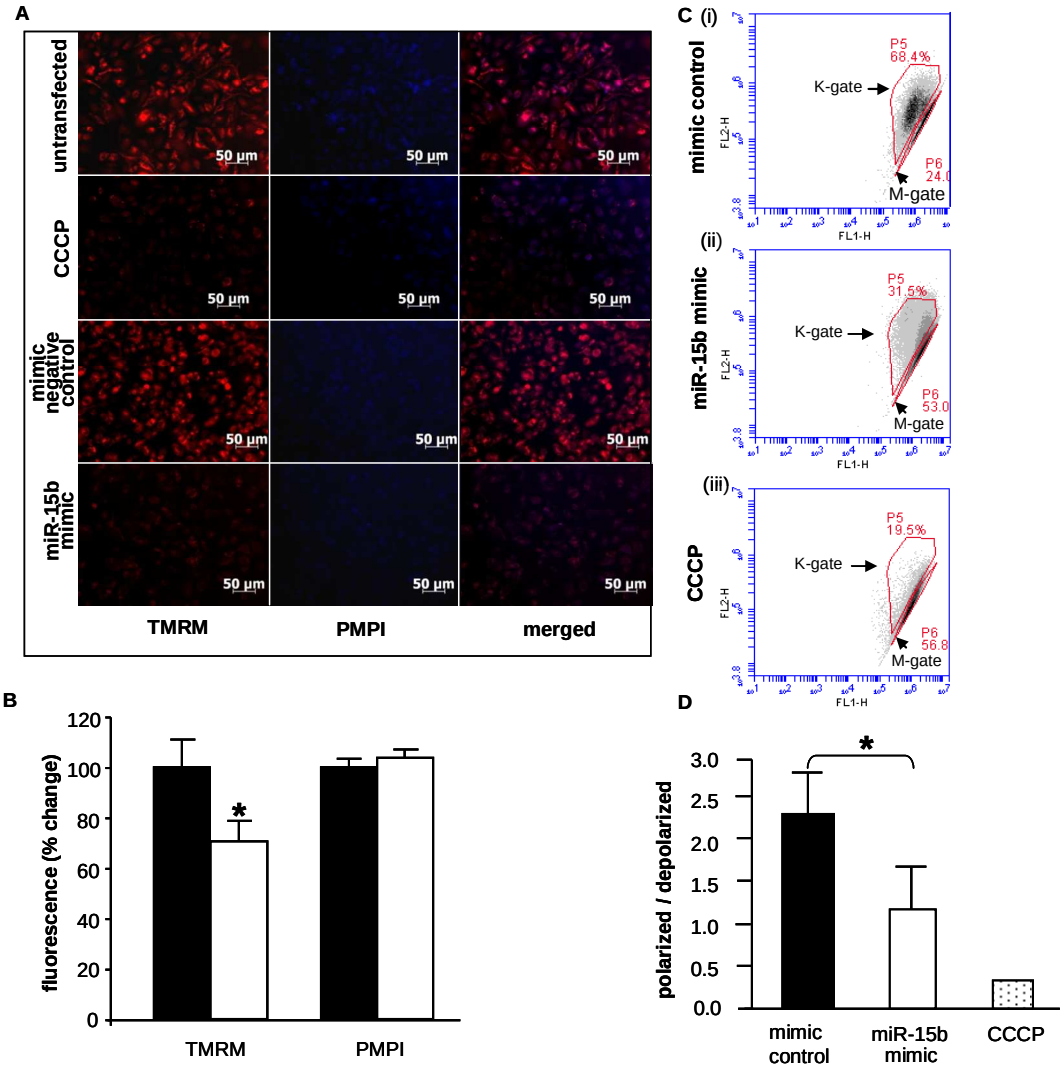

Figure 3. (A) Transfection of HL-1 cardiomyocytes with miRNA-15b mimic compromised mitochondrial membrane potential. HL-1 cells were transfected (72 hours) with mimic negative control or miRNA-15b mimic. Untransfected cells were used as negative control and cells transfected with carbonyl cyanide m-chlorophenylhydrazone (CCCP) were used as positive control (left panel – 8 nM tetramethylrhodamine methyl ester (TMRM); center panel - 0.5µl/ml plasma membrane potential indicator (PMPI); right panel - merged image). **(B)** Bar graph shows significant decrease in TMRM with no change in PMPI. Solid bars represent mimic negative control while open bars represent miRNA-15b mimic. **(C)** Loss of mitochondrial membrane potential in HL-1 cells transfected with miRNA-15b mimic, as assessed by JC-1 flow cytometry 72 h post-transfection. Cells were transfected with a (i) mimic control, (ii) miRNA-15b mimic or (iii) treated with CCCP Arrows (K gate) indicate cells containing JC-1 aggregates resulting from intact mitochondria; M gate indicates cells with low or collapsed mitochondrial membrane potential. **(D)** Ratio of polarized to depolarized cells calculated as a ratio between cells in K gate to M gate. Data indicate decrease in membrane potential upon up-regulation of miRNA-15b. Data expressed as mean ± SD (n=3).

***Dicer* deletion in the adult heart led to mitochondrial dysfunction and oxidative stress**

Redox state of the *Dicer* deleted adult heart was determined by EPR spectroscopy. After intramuscular injection of 2, 2, 5, 5,-tetramethylpyrrolidine-1-oxyl-3-carboxylic acid (PCA) to the heart, decay of nitroxyl radicals was studied (Figures 4A and supplementary figure S1A-B). A faster decay in *Dicer* deleted hearts was seen that has been considered indicative of a higher abundance of reactive oxygen species[8] (Figure 4B, $p<0.05$, n=3). This observation was consistent with elevated lipid peroxidation (Figure 4C; $p<0.05$, n=3) and glutathione oxidation (Figure 4D; $p<0.05$, n=4), indices of oxidative stress, in the hearts of $Dicer^{-/-}$ mice. These observations led to the hypothesis that the heart of $Dicer^{-/-}$ mice suffers from mitochondrial dysfunction resulting in oxidative stress. Analysis of respiration of isolated heart mitochondria led to the observation that the respiratory control ratio (RCR) was significantly decreased ($p<0.05$, n=5) in cardiac mitochondria from $Dicer^{-/-}$ mice compared with $Dicer^{+/+}$ animals (Figure 4E). Consistent with this observation demonstrating impairment in oxidative metabolism it was noted that lactate levels in the heart of $Dicer^{-/-}$ mice were significantly higher (Figure 4F; $p<0.05$, n=4). Taken together, these findings demonstrate that *Dicer* deletion induced hypertrophy and loss of cardiac function of the adult heart is associated with mitochondrial dysfunction and oxidative stress.

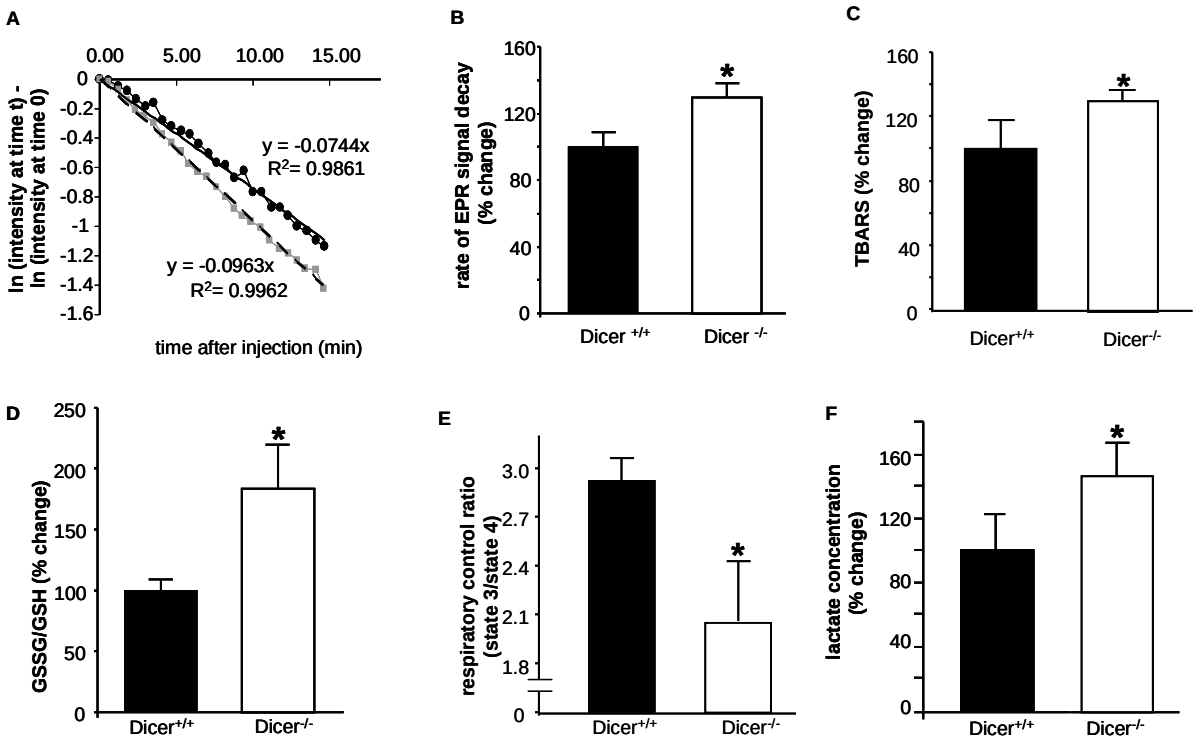

Figure 4. (A) Time course of average % signal change in the region of interest (ROI). Logarithmic values of signal change (normalized to the initial signal at time=0) in the ROIs are plotted with respect to time. Decay rate constants were obtained from the slope of linear decay after peak. Line with black circles represent Dicer$^{+/+}$ and line with grey circles represent Dicer$^{-/-}$. **(B)** Bar-graph showing the measured rate constants of nitroxide reduction in the tissues. Data expressed as mean ± SD (n=3). **(C)** Thiobarbituric acid–reactive substances (TBARS), an indicator of lipid peroxidation was measured from Dicer$^{+/+}$ and Dicer$^{-/-}$ hearts and was significantly higher in the later. Data expressed as mean ± SD (n=3) **(D)** Total GSSG to GSH ratio in Dicer$^{+/+}$ mice heart compared to Dicer$^{-/-}$ heart. Higher ratio indicates increased oxidative stress. Data expressed as mean ± SEM (n=3). **(E)** Respiratory coupling ratio (RCR) was significantly lower in Dicer$^{-/-}$ mice indicating mitochondrial dysfunction. Data expressed as mean ± SD (n=3). **(F)** Lactate levels measured in Dicer$^{+/+}$ and Dicer$^{-/-}$ mice hearts. Lactate is significantly higher in Dicer$^{-/-}$ mice. Data expressed as mean ± SD (n=3).

DISCUSSION

Dicer deficiency is emerging as a key factor determining health outcomes in humans. Cardiac-specific deletion of *Dicer* leads to defects in heart development and embryonic lethality[1, 4]. Loss of Dicer in the juvenile as well as adult myocardium induces hypertrophy, myofiber disarray, ventricular fibrosis and functional defects[3]. However, the underlying mechanisms remain unclear.

The current work capitalizes on the observation that the onset of cardiac pathologies and dysfunction after conditional *Dicer* deletion in adult hearts is rapid such that overt functional deficiencies are manifested in the first week. miRNA profiling performed at such early time-point helped identify the primary factors underlying cardiac dysfunction following *Dicer* deletion. The successful use of such information to develop a miRNA-based strategy to significantly rescue hearts from pathological changes caused by *Dicer* deletion provides first definitive evidence identifying a key miRNA-dependent pathway implicated in cardiac hypertrophy and dysfunction. Overt oxidative stress in Dicer-deficient hearts evident in this study pointed towards underlying mitochondrial dysfunction[24-25]. Indeed, studies with isolated mitochondria detected compromised RCR of mitochondria from Dicer-deficient hearts. ANTs export mitochondrial ATP into the cytosol and loss of ANT-1 expression has been recognized as a marker for mitochondrial dysfunction resulting in early cardiac dysfunction with later dilation and heart failure[26]. Our observation demonstrating lower ANT-1 in Dicer depleted hearts, support mitochondrial dysfunction as an underlying pathology. Mitochondrial energy deficiency is known to underlie dilated cardiomyopathy characterized by early mechanical dysfunction followed by a decline in left ventricular systolic function[26]. Hypertrophy and cardiac failure has often been associated with mitochondrial dysfunction and oxidative stress[24, 27-29]. The observation that *Dicer*-deletion in the adult heart caused early onset mitochondrial dysfunction led to the search for miRNA-dependent pathways targeting mitochondrial function in the heart. As we screened for miRNAs targeting mitochondrial function, elevated miRNA-15b emerged as a key candidate which is not only known to disrupt mitochondrial function Elevated miRNA-15b may also disrupt mitochondrial integrity by silencing ADP-ribosylation factor-like 2 (Arl2) therefore compromising cellular ATP levels[30]. Of interest, high miRNA-15b is known to be

associated with most common types of human heart failure[5-6]. Rescue experiments demonstrating that suppression of the rise of miRNA-15b in *Dicer*-deleted adult hearts result in marked amelioration of cardiac dysfunction definitively suggested a central role of miR-15b in determining cardiac mass and function. The significance of this observation is heightened by the reports demonstrating that miRNA-15b is elevated in most types of human heart failure[5-6]. Thus this study establishes the unique significance of miRNA-15b in determining cardiac metabolism and function. Interestingly, strategies to antagonize elevated miRNA-15b in the ailing heart may represent an efficient therapeutic approach which is worthy of consideration for clinical development.

ACKNOWLEDGMENT
Supported by R01 awards HL073087 and GM069589 to CKS.

REFERENCES:

1. Zhao Y, Ransom JF, Li A, Vedantham V, von Drehle M, Muth AN, Tsuchihashi T, McManus MT, Schwartz RJ, Srivastava D. Dysregulation of cardiogenesis, cardiac conduction, and cell cycle in mice lacking miRNA-1-2. *Cell.* 2007;129(2):303-317.
2. Saxena A, Tabin CJ. miRNA-processing enzyme Dicer is necessary for cardiac outflow tract alignment and chamber septation. *Proc Natl Acad Sci U S A.*107(1):87-91.
3. da Costa Martins PA, Bourajjaj M, Gladka M, Kortland M, van Oort RJ, Pinto YM, Molkentin JD, De Windt LJ. Conditional dicer gene deletion in the postnatal myocardium provokes spontaneous cardiac remodeling. *Circulation.* 2008;118(15):1567-1576.
4. Chen JF, Murchison EP, Tang R, Callis TE, Tatsuguchi M, Deng Z, Rojas M, Hammond SM, Schneider MD, Selzman CH, Meissner G, Patterson C, Hannon GJ, Wang DZ. Targeted deletion of Dicer in the heart leads to dilated cardiomyopathy and heart failure. *Proc Natl Acad Sci U S A.* 2008;105(6):2111-2116.
5. Small EM, Frost RJ, Olson EN. MicroRNAs add a new dimension to cardiovascular disease. *Circulation.*121(8):1022-1032.
6. Divakaran V, Mann DL. The emerging role of microRNAs in cardiac remodeling and heart failure. *Circ Res.* 2008;103(10):1072-1083.
7. Gnyawali SC, Roy S, McCoy M, Biswas S, Sen CK. Remodeling of the ischemia-reperfused murine heart: 11.7-T cardiac magnetic resonance imaging of contrast-enhanced infarct patches and transmurality. *Antioxid Redox Signal.* 2009;11(8):1829-1839.
8. Zhu X, Zuo L, Cardounel AJ, Zweier JL, He G. Characterization of in vivo tissue redox status, oxygenation, and formation of reactive oxygen species in postischemic myocardium. *Antioxid Redox Signal.* 2007;9(4):447-455.
9. Khanna S, Biswas S, Shang Y, Collard E, Azad A, Kauh C, Bhasker V, Gordillo GM, Sen CK, Roy S. Macrophage dysfunction impairs resolution of inflammation in the wounds of diabetic mice. *PLoS One.* 2010;5(3):e9539.
10. Khanna S, Roy S, Ryu H, Bahadduri P, Swaan PW, Ratan RR, Sen CK. Molecular basis of vitamin E action: tocotrienol modulates 12-lipoxygenase, a key mediator of glutamate-induced neurodegeneration. *The Journal of biological chemistry.* 2003;278(44):43508-43515.
11. Khanna S, Roy S, Slivka A, Craft TK, Chaki S, Rink C, Notestine MA, DeVries AC, Parinandi NL, Sen CK. Neuroprotective properties of the natural vitamin E alpha-tocotrienol. *Stroke.* 2005;36(10):2258-2264.
12. Sen CK, Khanna S, Babior BM, Hunt TK, Ellison EC, Roy S. Oxidant-induced vascular endothelial growth factor expression in human keratinocytes and cutaneous wound healing. *The Journal of biological chemistry.* 2002;277(36):33284-33290.
13. Chen YR, Chen CL, Pfeiffer DR, Zweier JL. Mitochondrial complex II in the post-ischemic heart: oxidative injury and the role of protein S-glutathionylation. *The Journal of biological chemistry.* 2007;282(45):32640-32654.
14. Crouser ED, Julian MW, Blaho DV, Pfeiffer DR. Endotoxin-induced mitochondrial damage correlates with impaired respiratory activity. *Crit Care Med.* 2002;30(2):276-284.
15. Claycomb WC, Lanson NA, Jr., Stallworth BS, Egeland DB, Delcarpio JB, Bahinski A, Izzo NJ, Jr. HL-1 cells: a cardiac muscle cell line that contracts and retains phenotypic characteristics of the adult cardiomyocyte. *Proc Natl Acad Sci U S A.* 1998;95(6):2979-2984.

16. Shilo S, Roy S, Khanna S, Sen CK. Evidence for the involvement of miRNA in redox regulated angiogenic response of human microvascular endothelial cells. *Arterioscler Thromb Vasc Biol.* 2008;28(3):471-477.

17. Hussain SR, Cheney CM, Johnson AJ, Lin TS, Grever MR, Caligiuri MA, Lucas DM, Byrd JC. Mcl-1 is a relevant therapeutic target in acute and chronic lymphoid malignancies: down-regulation enhances rituximab-mediated apoptosis and complement-dependent cytotoxicity. *Clin Cancer Res.* 2007;13(7):2144-2150.

18. Reid AB, Kurten RC, McCullough SS, Brock RW, Hinson JA. Mechanisms of acetaminophen-induced hepatotoxicity: role of oxidative stress and mitochondrial permeability transition in freshly isolated mouse hepatocytes. *J Pharmacol Exp Ther.* 2005;312(2):509-516.

19. Khanna S, Roy S, Parinandi NL, Maurer M, Sen CK. Characterization of the potent neuroprotective properties of the natural vitamin E alpha-tocotrienol. *J Neurochem.* 2006;98(5):1474-1486.

20. Roy S, Biswas S, Khanna S, Gordillo G, Bergdall V, Green J, Marsh CB, Gould LJ, Sen CK. Characterization of a preclinical model of chronic ischemic wound. *Physiol Genomics.* 2009;37(3):211-224.

21. Roy S, Khanna S, Rink C, Biswas S, Sen CK. Characterization of the acute temporal changes in excisional murine cutaneous wound inflammation by screening of the wound-edge transcriptome. *Physiol Genomics.* 2008;34(2):162-184.

22. Roy S, Patel D, Khanna S, Gordillo GM, Biswas S, Friedman A, Sen CK. Transcriptome-wide analysis of blood vessels laser captured from human skin and chronic wound-edge tissue. *Proc Natl Acad Sci U S A.* 2007;104(36):14472-14477.

23. Sohal DS, Nghiem M, Crackower MA, Witt SA, Kimball TR, Tymitz KM, Penninger JM, Molkentin JD. Temporally regulated and tissue-specific gene manipulations in the adult and embryonic heart using a tamoxifen-inducible Cre protein. *Circ Res.* 2001;89(1):20-25.

24. Tsutsui H, Ide T, Kinugawa S. Mitochondrial oxidative stress, DNA damage, and heart failure. *Antioxid Redox Signal.* 2006;8(9-10):1737-1744.

25. Miyamoto S, Murphy AN, Brown JH. Akt mediates mitochondrial protection in cardiomyocytes through phosphorylation of mitochondrial hexokinase-II. *Cell Death Differ.* 2008;15(3):521-529.

26. Narula N, Zaragoza MV, Sengupta PP, Li P, Haider N, Verjans J, Waymire K, Vannan M, Wallace DC. Adenine nucleotide translocase 1 deficiency results in dilated cardiomyopathy with defects in myocardial mechanics, histopathological alterations, and activation of apoptosis. *Jacc.*4(1):1-10.

27. Seddon M, Looi YH, Shah AM. Oxidative stress and redox signalling in cardiac hypertrophy and heart failure. *Heart.* 2007;93(8):903-907.

28. Tsutsui H. Mitochondrial oxidative stress and heart failure. *Intern Med.* 2006;45(13):809-813.

29. Dhalla AK, Hill MF, Singal PK. Role of oxidative stress in transition of hypertrophy to heart failure. *J Am Coll Cardiol.* 1996;28(2):506-514.

30. Nishi H, Ono K, Iwanaga Y, Horie T, Nagao K, Takemura G, Kinoshita M, Kuwabara Y, Mori RT, Hasegawa K, Kita T, Kimura T. MicroRNA-15b modulates cellular ATP levels and degenerates mitochondria via Arl2 in neonatal rat cardiac myocytes. *The Journal of biological chemistry.*285(7):4920-4930.